Blind Deconvolution of Camera Motioned Picture using Depth Map

B.Kalaiyarasi[1], S.Kalpana[2]
II-M.E(CS)[1], AP / ECE[2], Dhanalakshmi Srinivasan Engineering College, Perambalur.
Dhanalakshmi Srinivasan Engineering College, Perambalur.

Abstract — **Camera shake leads to non-uniform image blurs for large depth range scene and apparent camera translation. To restore the blurred images of large-depth range scenes attenuated by camera motion, we build an arbitrary model 6-degree of freedom (DoF) of camera motion with a depth map. In this paper we have done a successful blind deconvolution for removing shake artifacts that requires the estimation of a spatially varying or non-uniform blur operator using iterative deblurring algorithm. The number of variables is reduced by time sampling motion function (TSMF), which describes the 6-DoF camera motion by sampling the camera position in time domain. To effectively estimate the high-dimensional camera motion parameters, we construct the probabilistic motion density function (PMDF) to describe the camera poses during exposure, and the convergence of the deblurring algorithm. Specifically, PMDF is computed through a back projection method from 2D local blur kernels to 6D camera motion and robust voting. For the degeneration situations, our framework can flexibly select the motion dimension to degrade the motion blur model, and thus can reduce computational cost and prevent over-fitting.**

Index Terms— **Blind deconvolution, camera shake, depth map, depth dependent, non-uniform blur.**

I INTRODUCTION

Motion blur due to camera motion can significantly degrade the quality of an image. Since the path of the camera motion can be arbitrary, deblurring of motion blurred images is a hard problem. The effect of a particular camera shake can be described by a linear transformation on the sharp image, i.e., the image that would have been recorded using a tripod. Denoting for simplicity images as column vectors, the recorded blurry image y can be written as a linear transformation of the sharp image x, i.e., as y = Ax, where A is an unknown matrix describing the camera shake. Regular linear and non-linear deconvolution techniques utilize a known PSF. For blind deconvolution, the PSF is estimated from the image or image set, allowing the deconvolution to be performed. Blind deconvolution can be performed iteratively, whereby each iteration improves the estimation of the PSF and the scene, or non-iteratively, where one application of the algorithm, based on exterior information, extracts the PSF. A good estimate of the PSF is helpful for quicker convergence but not necessary. Blind deconvolution has several challenging aspects: modeling the image formation process, formulating tractable priors based on natural image statistics, and devising efficient methods for optimization.

RELATED WORKS:

The works on camera shake removal fall into two main streams according to the assumption on blur kernels: spatially uniform and non-uniform. The former methods formulate image blur as a 2D convolution process, and perform deconvolution on a single blurred image, multiple images, captured at different settings such as long-exposure/short exposure image pair or an image set deteriorated by different blur kernel. The uniform methods assume that all the pixels are blurred with the same blur kernel, but this assumption does not hold because the image blur at a specific position is highly correlated with both camera motion and corresponding scene depth, i.e., spatially varying.

The spatial variance of Point Spread Functions (PSFs) are correlated with two types of camera motion, rotation and translation, between which the spatial variance caused by rotation is depth independent, while that caused by translation heavily depends on scene depth. Taking both translation and rotation into consideration, use inertial sensors to measure the 6-DoFs camera motion, and perform image deblur subsequently. Without external input, use in-plane rotation and *x*, *y*-translation to approximate the 6-DoF motion to reduce computational cost and use a blind deblur algorithm to

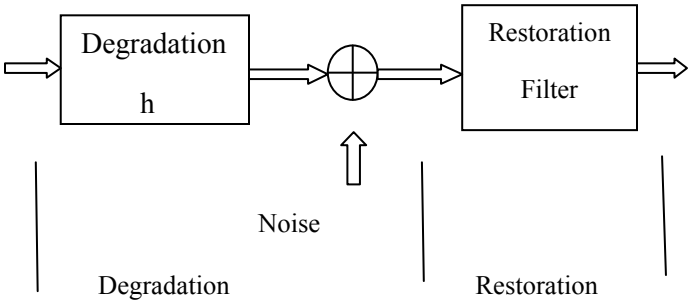

Fig.1. Image restoration model

ISSN: 2278 – 909X

restore the sharp image. Fig.1 shows the general image restoration process. Furthermore, an efficient-filter-flow based deblurring framework which can deal with both rotation and translation combine the image restoration algorithm with Simultaneous Localization And Mapping (SLAM) technique to solve their 6-DoF motion blur model which assumes that the local blur kernels are straight lines. In spite that being able to handle both camera rotation and translation and give promising results, there are two major limitations to above methods: firstly, they either depend on external input (hardware or user interaction) for camera motion estimation/acquisition or simplify the motion parameters to avoid intensive computation; secondly, most of the above blur models assume planar scenes.

II.OUR APPROACH AND PAPER ORGANIZATION

To deal with the non-uniform blur caused by an arbitrary camera motion, both scene structure and high-dimensional motion need to be considered. In this paper, we use a depth aware projective blur model considering scene depth and describe motion with 6 DoF explicitly. Practically, scene structure can be acquired by a depth camera or computed by structure from X approaches, while computing high dimensional motion parameters will severely intensify the computation cost, which is a common problem in non-uniform deblurring. Actually, computing 6-DoF motion parameters using traditional methods is intractable, so most of the existing methods simplify the motion blur model to lower DoF to approximate the 6D camera motion. To the best of our knowledge, state-of-the-art blind deblurring approaches can only handle camera motion of no higher than 3 DoF, which limits the capacity of these algorithms for dealing with the image of large-depth-range scenes deteriorated by 6D camera motion.

To overcome this problem, Temporal Sampling Motion Function (TSMF) and Probabilistic Motion Density Function (PMDF) are proposed to reduce variable number and improve the convergence respectively.

1) TSMF: Traditional blind deblurring methods use the probability density function of motion parameter to describe the camera motion by sampling uniformly in parameter space and giving each sample a weight to describe the fraction of time the camera spent on this discretized pose. As the parameter dimension increases, the needed sample size increases drastically and induces high computational cost. In addition, because camera trajectory is just a 1D curve in the 6D parameter space, most of the samples in parameter space are trivial (zero entries), which implies that this sampling method is inefficient. Furthermore, since the sparsity constraint of the motion has to be used to regularize the problem, this will further intensify the computation cost. To address this problem, TSMF is proposed to describe camera motion by sampling camera poses in time-domain and each sample needs at most 6 parameters to describe the camera pose at this moment. Without sampling in the triviality area of parameter space, TSMF is much more efficient and thus reduces the variable number considerably.

2) PMDF: Deblurring approaches usually optimize camera motion and latent sharp image iteratively, however, the convergence of high-dimensional motion blur model is very difficult. In this paper, PMDF is adopted to constrain the motion parameters and thus improves convergence of optimization. In computation aspect, we propose to compute PMDF by a robust voting framework from low-dimensional blur kernels, which can be estimated from local image patches. In practice, we describe the PMDF in a probabilistic manner instead of an exact optimum to raise the robustness to estimation error of low-dimensional blur kernels.

This paper firstly describes the adopted imaging model and parametrization (TSMF) and then gives the two steps of our algorithm respectively:

1) Compute PMDF
   a) Split image into patches and estimate their 2D local blur kernels
   b) Calculate the confidence of 2D local blur kernels
   c) Project 2D local blur kernels back to 6D parameter space and estimate PMDF by robust voting
2) PMDF guided camera shake removal
   a) Add PMDF to objective function as a constraint
   b) Iteratively optimize TSMF and sharp image

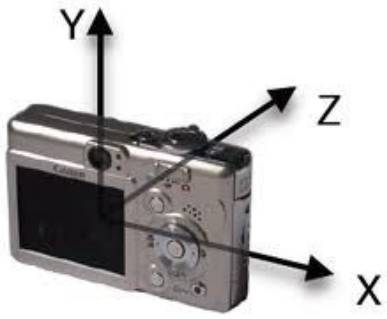

Fig.2. Diagram of general camera projective blur model

In summary, the proposed model is advantageous over the Previous methods in multiple aspects:

(i) Depth and 6-DoF camera motion are both explored explicitly to address arbitrary motion blur for large depth range scene

(ii) Camera motion is modeled completely with 6 DoF, and TSMF is proposed to reduce the scale of the problem effectively

(iii) PMDF is proposed to impose unified constraints to spatially varying blur, and it can be computed effectively from low-dimensional local kernel estimation under a robust voting scheme.

Fig.3 depicts the 2 dimensional manifold analysis of a curve-like kernel obtained by the projective blur model by translation and rotation process.

ISSN: 2278 – 909X

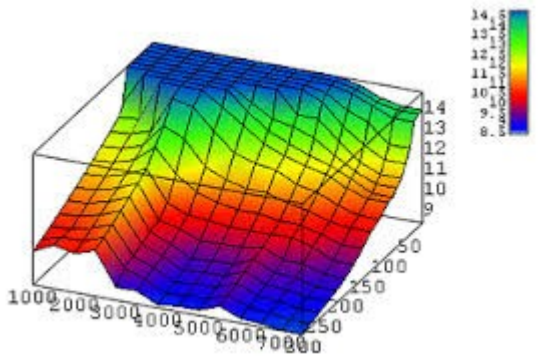

Fig.3: 2D mapping manifold of a curve-like kernel

III ALGORITHM AND TECHNIQUES DETAILS

PDMF ALGORITHM

Camera motion estimation in blind deblurring is a nonconvex problem, and it becomes more difficult to solve when the dimension of parameter space grows. To estimate the high-dimensional (> 2) motion by projecting low-dimensional projections (2D kernel) back to high-dimensional motion parameter space. Considering the estimation error of 2D kernel a Probabilistic Motion Density Function (PMDF) which represents the probability distribution of camera motion in high-dimensional parameter space is estimated. The 3D PMDFs are represented by 3D cubes with different density in different colors, and each cube in the 3D space corresponds to a tuple of motion parameters.

A. Patch-Based Local 2D Kernels Estimation & Confidences

Uniformly crop overlapping image patches with constant patch size from the input blurred image to estimate local blur kernels. The patch size can be determined according to the camera intrinsic and maximum motion range by considering the rotation caused non-uniformity. The overlap size is set to be slightly larger than the maximum 2D kernel size. The fast deblurring algorithm is applied to the patches to estimate the local blur kernels. From coarse to fine scales, the bilateral and shock filters are used to predict the latent image, followed by the kernel estimation and deconvolution. Uniform deblurring algorithms can be used to replace the adopted algorithm. Each patch is given a confidence according to its intensity and depth by considering the translation caused non-uniformity.

1) Size of Patches:

Generally, conventional deblurring methods work better in bigger patches. However, considering the non-uniformity of blur kernels within a single patch is not efficient. Limit the patch size to ensure that the uniform assumption can approximate the real case well. Because translation caused non-uniformity mainly depends on scene structure rather than patch size, discuss rotation caused non-uniformity here.

According to the camera intrinsic and range of rotation parameters, we can determine the maximum patch size under a certain tolerance of non-uniformity within a patch. The non- uniformity metric between two point spread trajectories $\mathbf{x}\_(t)$ and $\mathbf{y}\_(t)$ at coordinate **x** and **y** respectively, then the metric can be defined .

2) Confidence of Patches:

There are two main factors affecting the accuracy of estimated local blur kernels: richness of texture and uniformity of blur kernels within the patch. The confidence of estimated local blur kernels is calculated according to these two factors.

a) Richness of texture:

It is reasonable that blur kerne estimated from a local image patch with abundant texture should be more creditable than that from textureless patch. The traditional texture measurements like image entropy or Harris corner metric can be used in our scenario.

$$C_{H(patch)}=-\sum_{i,j} f_{i,j} \log f_{ij} \qquad (1)$$

where $f_{i,j}$ is the frequency of pixels in the patch with intensity being i and the mean value of its neighborhood being j .

b) Uniformity of blur kernels:

The rotation caused non-uniformity of local blur kernels can be constrained by reducing patch size; the spatial non-uniformity caused by translation should also be taken into consideration. Geometrically, the translation blur is depth dependent, so we favor the blur kernel estimated from a patch with consistent depth. The reciprocal of standard deviation of depth in the patch as metric of depth consistency is used.

$$C_d(patch)=1/\sqrt{\sum}(D(u,v)-D(u,v)) \qquad (2)$$

Confidence of the estimation accuracy is:

$$C(patch)=C_d(patch)C_H(patch) \qquad (3)$$

To reduce computational cost, the blocks with low confidence weights are removed by setting the truncation threshold adaptively to preserve at least 95% of the total confidences.

B. PMDF Estimation

For an arbitrary motion vector **M**, the $P_m(\mathbf{M})$ can be calculated by interpolation from discrete samples. Firstly,

ISSN: 2278 – 909X

Parameterization is done to form the sample set in high-dimensional motion parameter space, and then vote the mappings of local blur kernels in high-dimensional motion parameter space to compute PMDF.

1) *Parameterization:*

If *N* is the limit of 2D kerne size, which can be set according to the blur level of image, the projection of high-dimensional camera motion in 2D kernel space should be no larger than *N* To ensure estimation accuracy of PMDF, the 2D projection in imaging plane of each discrete level should be no larger than one pixel to eliminate ambiguity, consequently the number of discretization levels along each axis should be more than *N*. When the camera motion during exposure is slight, uniformly discretizing each parameter will lead to a near uniform sampling in 2D blur kernel space, i.e. the interval in 2D blur kernel domain between projections of two adjacent samples is approximately one pixel as well. To be on the safe side, set 1.2*N* discretization levels along each dimension.

2) *Back-Projection:*

The 2D local blur kernels can be regarded as the 2D projection of 6D camera motion. Inversely, for a certain 2D local blur kernel, there are a set of samples meeting the projection. The so-called back-projection step is trying to calculate this set and their corresponding weights for a certain local blur kernel.

3) Robust Voting:

In this step, the PMDF is computed by a weighted voting process. For each sample in high- dimensional parameter space, its probability density can be estimated by considering the contamination from bad hypotheses (i.e. outliers of 2D local blur kernels estimated by uniform method), we propose a robust voting method to compute PMDF. As is well known, median filter is widely used in robust estimation for its desirable ability in suppressing the effects from bad hypotheses, but it cannot deal with the white noise with short-tailed distribution. Therefore, we adopt order based bilateral weighted voting which combines median filter and Gaussian filter to achieve good performance under both bad hypotheses and short-tailed noise of good hypotheses Utilizing the PMDF to guide our non-uniform deblurring . The latent image by Maximum A Posteriori (MAP).

In the first iteration, the latent image **I** can be initialized by stitching deblurred patches. To suppress the bad deblurred results, the confidence map is used to weight each pixel. Considering the 2D blur kernel domain, since 2D kernels are projections of camera motion, it can be regarded as a summation of a series of impulse kernels which correspond to the camera poses along the camera motion trajectory. The Center of the impulse kernel locates at the pixel **x** and the peak value of the kernel has an offset $d\mathbf{x}$, which is used to transform the pixel **x** on latent image to its corresponding pixel $\mathbf{x}'$ on warped image, and we denote the offset as

$$d\mathbf{x} = \mathbf{x}' - \mathbf{x}. \quad (4)$$

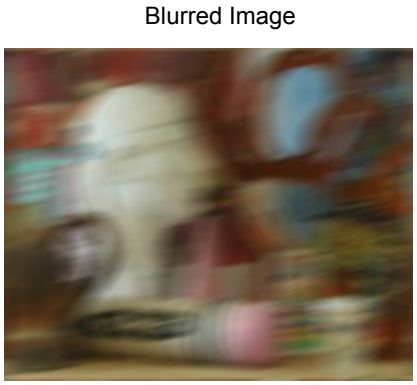

(a)

(b)

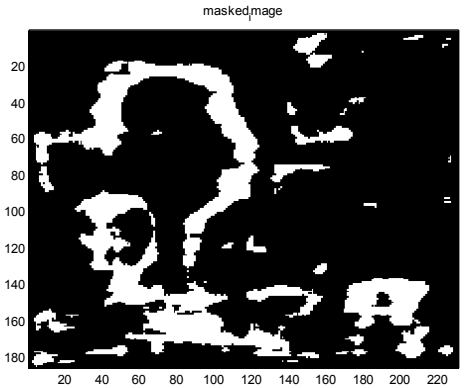

(c)

ISSN: 2278 – 909X

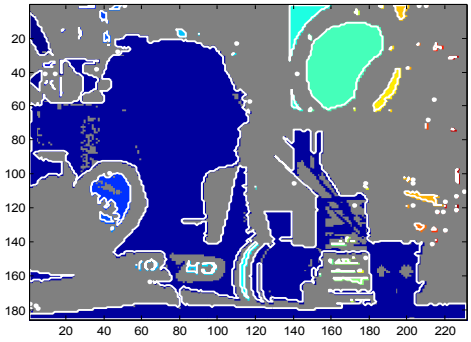

(d)

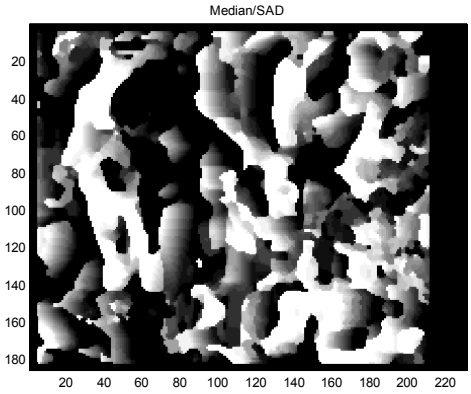

(e)

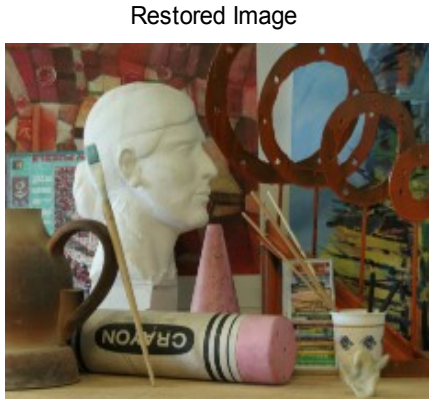

(f)

Fig.4: a) Blurred image b) image obtained after patching process c) masked image d) binary image e) filtration process f) restored image.

IV. ANALYSIS AND EXPERIMENTS

In this section, experiments are conducted to analyze the model parameters and validate the proposed algorithm.

A. Manifold Analysis

1) Impulse Kernel:

Considering the 2D blur kernel domain, since 2D kernels are projections of camera motion, it can be regarded as a summation of a series of impulse kernels which correspond to the camera poses along the camera motion trajectory. The center of the impulse kernel locates at the pixel **x** and the peak value of the kernel has an offset $d\mathbf{x}$, which is used to transform the pixel **x** on latent image to its corresponding pixel **x** on warped image, and we denote the offset as $d\mathbf{x} = \mathbf{x} - \mathbf{x}$. In the case of 2D impulse kernel, the peak point corresponds to a $N-2$ dimensional manifold in N dimensional parameter space. Specific to the 3D parameter space case, this manifold is 1D and can be embedded into 3D Euclidean space. We will show the mapping manifolds of these impulse kernels and analyze the effects of three variables **x**, $D(\mathbf{x})$ and $d\mathbf{x}$ on these manifolds respectively.

a) Kernel center **x***:* Kernel center **x** describes the location of the 2D local blur kernel and is also the center of corresponding pixel in latent image. Here we fix $d\mathbf{x}$ to be $(0, 0)$ and $D(\mathbf{x})$ to be 5m, and change **x** in both horizontal and vertical directions. The mapping manifolds in 3D parameter space which reveals that these 1D manifolds are almost straight lines when motion parameters vary with a small range around origin, while the slopes of these lines change as the kernel center **x** changes. However, all these manifolds intersect at the origin point which is the exact 3D motion parameters of camera pose coincide with these impulse kernels.

b) Depth $D(\mathbf{x})$*:* The mapping manifolds with different depths, with the kernel center **x** and offset $d\mathbf{x}$ being set constant. According to the figure, *the slopes of these 1D manifolds change with scene depth*. However, unlike **x**, their thicknesses also vary with depth. This is in accordance with the projective geometry, i.e. the farther the scene point is, the more translation is needed to cause the same offset in 2D blur kernel space, an extreme case is when the depth is infinite translation will never cause any movement of the projection. Therefore, a pixel with the same size in blur kernel domain corresponds to a thicker manifold in parameter space as the depth increases. As the scene point moved nearer, the projection range of the manifold on translation axes expands while that on rotation axes shrinks. We can conclude that large depth helps to determine rotation, and small depth helps to determine translation, and *the scene with large depth range is in favor for high-dimensional camera motion estimation.*

c) Offset $d\mathbf{x}$*:* Offset $d\mathbf{x}$ describes the shift of peak point of impulse kernel. For a certain scene point (i.e. the **x** and $D(\mathbf{x})$

ISSN: 2278 – 909X

are constant) *the varying of d***x** *corresponds to translation of the 1D mapping manifold on Tx , Ty directions* in 3D parameter space.

2) Continuous Kernel: One important property of motion blur kernel is the continuity, so that the kernel can be regarded as a trajectory of a moving speckle, with the velocity reflected by the intensity of pixels along the trajectory. As discussed above, the varying of offset *d***x** corresponds to translation of mapping manifold along *Tx , Ty* directions in 3D parameter space, so the 1D manifold spans to be a 2D surface in 3D parameter space. The points with the same color in the surface have the same probability motion density. We set **x** to be *(*0, 0*)* and *D(***x***)* to be 5m and give the surface manifold of the continuous kernel in 3D motion parameter space. The unknown camera motion trajectory is a curve along the surface from one side to the other. Furthermore, local blur kernels estimated from different kernel center and scene depths lead to different mapping surfaces, their intersection determines the 3D camera motion trajectory.

3) Parameter Space With Dimension Higher Than 3:
Although the above discussions are all based on the 3D parameter space, the conclusions can be extended to higher dimensional space:

(i) 2D blur kernels estimated from each patch are projected from the common camera motion, so the intersection of their projection in high-dimensional space fits the camera motion trajectory

(ii) Big scene depth (i.e. farther scene) helps to determine camera rotation parameters, while small scene depth (i.e. nearer scene) helps to determine translation. Thus, large depth range scene helps to determine the unknown camera motion, and small depth range may lead to model degeneration, i.e. the problem has multi-solutions.

(iii) Incremental shift between latent image and blurred image reflects the movement of mapping manifold along translation directions (*x*−, *y*− axes).

B. Analysis of Depth-Dependent Blur

Here, we analyze some characteristics of depth-dependent blur caused by camera translation.

1) Sensitivity to Sudden Depth Change: Both translation and rotation may cause non-uniform blur, however, the rotation blur varies gradually over the image, so it is possible to find a single PSF with sufficient accuracy for a small local region, and obtain promising deblurring results by deconvolution. In contrast, the translation blur changes significantly at the step edges that reflect discontinuous scene depth, and ignoring the abrupt change of PSFs at these positions would deteriorate the deblurring performance by introducing or aggravating ringing artifacts. Therefore, compared with the rotation, the blur caused by translation is more challenging in image deblurring.

2) Over-Deblurring & Under-Deblurring: Although translation blur varies with scene depth, the general shape of the PSFs is preserved. Therefore, inaccurate estimation of PSFs due to translation may result in two possible undesired outcomes: over-deblurring and under-deblurring, i.e., deblurring using a kernel larger and smaller than the actual size. we can conclude that the smaller blur kernel leads to incomplete deblurring, while the larger one introduces apparent ringing artifacts. Therefore, *depth-dependent blur kernel must be considered* to remove the non-uniform blur while suppress the ringing artifacts along depth edges.

C. Experiment Results With Given Depth Map

1) Image Deblurring With Synthetic Depth and Motion:

We select an image with large depth range and blur it by a simulated 6D camera motion and intrinsics. To show the effectiveness of the global constraint, we demonstrate the result of a naive fix-size-patch non-uniform deblurring algorithm with the same patch size as our method. For each patch, a state-of-the-art uniform method is applied. Considering that the size of the blurred image is relatively small (383×434 pixels) compared to the patch size (100×100 pixels), this experiment is very challenging for our patch based framework. Obviously, our approach gives promising results in all the regions while the other methods fail in some regions, because neither depth is considered nor the adopted motion model can approximate the 6D camera motion well enough.

To test the tolerance of the proposed method to depth inaccuracy, we applied our algorithm on the depth estimated from the multiviews. One can notice that the performance is slightly affected but still quite promising compared to that given true depth. The robustness to depth inaccuracy is mainly due to the proposed weighted voting strategy.

2) Image Deblurring With Depth Camera Assistance:

To display the integral performance of the whole framework, we test our deblurring algorithm on data captured by a RGB/depth hybrid acquisition system. It is obvious that the uniform algorithms perform well in the selected region while the performances in other areas deteriorate. On the contrary, we achieve good performance over the whole image.

3) Image Deblurring With Depth Computed by Structure From Motion Method:

In practical applications, depth acquisition equipment may not be easily available for some scenarios. Fortunately, our methods do not need a high quality depth map, so we can use the depth map derived by structure from motion methods. To deal with the feature correspondence between blurred images, we down sample the original blurred image to derive the coarse depth map and then smooth it by bilateral filtering after up sampling.

ISSN: 2278 – 909X

V .CONCLUSION

We have proposed a 6D depth-aware blur model and an effective camera motion estimation technique. From the guidance of unified camera motion distribution estimated by local blur information; our method achieves good deblurred result for non-uniformly blurred images, especially in the situations with large depth range scene and apparent camera translation. For the degeneration situations, our framework can flexibly select the motion dimension to degrade the motion blur model, and thus can reduce computational cost and prevent over-fitting. This paper also proposes back projection and weighted voting technique to raise the robustness to estimate the errors in some extreme cases. As shown in the experiments, our algorithm can give promising result when most estimated local blur kernels have intensive errors and noise. However, the accuracy of locally estimated blur kernels is still crucial for our framework. In future scope, this deblurring model can be improved by applying Poisson deblurring algorithm with Gaussian filter to the blurred image to obtain a sharp image. In the future, we'll also try to improve the algorithm to be more robust and adaptive. In terms of computational speed, it can be greatly accelerated by GPU for most calculations within each iteration are highly parallel. In addition, out-of-focus effect will also be considered as an extension.

REFERENCES

[1] High-Dimensional Camera Shake Removal With Given Depth Map Tao Yue, Jinli Suo, and Qionghai Dai, *Senior Member, IEEE, IEEE* TRANSACTIONS ON IMAGE PROCESSING,VOL.23,NO.6,JUNE 2014

[2] L. Xu and J. Jia, "Depth-aware motion deblurring," in *Proc. ICCP*, 2012, pp. 1–8.

[3] H. Zhang, J. Yang, Y. Zhang, N. Nasrabadi, and T. Huang, "Close the loop: Joint blind image restoration and recognition with sparse representation prior," in *Proc. IEEE ICCV*, Nov. 2011, pp. 770–777.

[4] D. Zoran and Y. Weiss, "From learning models of natural image patches to whole image restoration," in *Proc. IEEE ICCV*, Nov. 2011, pp. 479–486.

[5] X. Chen, X. He, J. Yang, and Q. Wu, "An effective document image deblurring algorithm," in *Proc. CVPR*, 2011, pp. 369–376.

[6] S. Cho, J. Wang, and S. Lee, "Handling outliers in non-blind image deconvolution," in *Proc. ICCV*, 2011, pp. 1–8.

[7] W. Li, J. Zhang, and Q. Dai, "Exploring aligned complementary image pair for blind motion deblurring," in *Proc. CVPR*, 2011, pp. 273–280.

[8] U. Schmidt, K. Schelten, and S. Roth, "Bayesian deblurring with integrated noise estimation," in *Proc. CVPR*, 2011, pp. 2625–2632.

[9] A.Letouzey, B. Petit, E. Boyer, and M. Team, "Scene flow from depth and color images," in *Proc. BMVC*, 2011, pp. 46-1–46-11.

[10] J. Shotton *et al.*, "Real-time human pose recognition in parts from single depth images," in *Proc. CVPR*, 2011, pp. 1297–1304.

[11] Y. Tai, N. Kong, S. Lin, and S. Shin, "Coded exposure imaging for projective motion deblurring," in *Proc. CVPR*, 2010, pp. 2408–2415.

[12] A.Gupta, N. Joshi, C. L. Zitnick, M. F. Cohen, and B. Curless, "Single image deblurring using motion density functions," in *Proc. 11th ECCV*, 2010, pp. 171–184

[13] N. Joshi, S. Kang, C. Zitnick, and R. Szeliski, "Image deblurring using inertial measurement sensors," *ACM Trans. Graph.*, vol. 29, no. 4, pp. 1–8, Jul. 2010.

[14] S. Zhuo, D. Guo, and T. Sim, "Robust flash deblurring," in *Proc. CVPR*, 2010, pp. 2440–2447.

Kalaiyarasi received the B.E degree in Electronics and Communication Engineering from Anna University, India in 2013. She is currently pursuing M.E degree in Communication Systems, Anna University, India. Her research interests mainly include image processing and computational photography.

Kalpana received the B.E degree in Electronics and Communication Engineering from Anna University, India and the M.E degree in Communication Systems, Anna University, India. She is currently working as an assistant professor in the department of ECE, Dhanalakshmi Srinivasan Engineering College, Perambalur. Her research interests mainly include digital communication, image processing and computational photography.

ISSN: 2278 – 909X